

## **PERFORMANCE ASSESSMENT OF STEEL MOMENT CONNECTIONS RETROFITTED WITH VARIOUS REDUCED SECTION PATTERNS**

Abbas SIVANDI-POUR<sup>1</sup>

Faculty of Civil and Surveying Engineering,  
Graduate University of Advanced Technology, Kerman, Iran

### **A b s t r a c t**

It is of high importance in seismic retrofitting of lateral load-bearing systems to increase the connections performance. The crucial point in the steel frame retrofitting process is to create plastic hinges in these types of frames. The formation of plastic hinges in beams and near columns generates large strains on column flanges as well as welding metal and heated surroundings, which can lead to brittle failure. The connection should be designed in such a way as to allow plastic hinge formation at certain points of the beam. One such method suggested for retrofit connections is to reduce the beam section locally away from the connection zone. There are various patterns available to locally reduce the beam section, such as circular, elliptical, and symmetric/asymmetric. In recent years, different proposals have been presented to design these connections which vary from older instructions. For this study, radiused cuts in the flange and slotted holes in the web of connection beams were selected for retrofitting analysis. Cyclic behavior, energy damping levels, and ductility of these connections were studied and compared before and after the retrofit by using nonlinear dynamic analysis. The results showed that the symmetrical circular hole pattern in the beam flanges demonstrated reliable performance.

**Keywords:** reduced beam sections, energy damping, cyclic behavior, nonlinear analysis

---

<sup>1</sup> Corresponding author: Graduate University of Advanced Technology, Faculty of Civil and Surveying Engineering, Kerman, Iran, e-mail: a.sivandi@kgut.ac.ir

## 1. INTRODUCTION

Earthquake loads, after being distributed by a solid slab, are transferred to the columns through the connections in moment frames systems and also elements like bracing and shear walls in other frame systems. Besides, the seismic strength of steel moment frames is highly reliant on the quality of the connections and the connection method between beams and columns. Increasing connection performance is extremely important in seismic retrofitting of lateral load resisting frames. Studies on connection behavior during earthquakes show severe damage to the structure is caused by plastic hinge formation near the columns and in the connection area (Chi et al., 2006; Gerami et al., 2013; Sivandi-Pour et al., 2014; Farsangi et al., 2016; Farsangi; et al., 2018; Bogdanovic A. et al., 2019). Various methods have been suggested to avoid this problem, one of which is the addition of elements to the connection in order to increase the beam strength and reduce connection stress. In another method, using reduced beam sections (RBS) with various patterns is suggested to increase the seismic performance of the connections as, by using this method, there will be a plastic zone in a pre-defined area. Due to yielding of the beam flange and formation of a plastic hinge in the pre-defined area, a great amount of seismic loading will be dissipated and, thus, connection ductility increases. Under the lateral loading and nonlinear deflections in the frames, multiple plastic hinges form. The connections must be retrofitted in such a way as to allow these formations to be concentrated in certain parts of the beam and also reliable enough to move the plastic hinge far enough from the column. One influential parameter in the connection retrofitting procedure is increasing the strength of the panel zone and there has been plenty of research into the effects of panel zones and RBS connections on seismic behavior of steel structures (Jones et al., 2002; Lee et al., 2005; Han et al., 2009; Tuna and Topkaya, 2015; Rong et al., 2018). Yang et al. studied the behavior of steel frames with reduced web section beams experimentally. Their results showed that the presence of an opening in the web of the moment frame will satisfy the seismic needs while also not diminishing the frame stiffness. The nonlinear behavior of a frame with reduced beam sections illustrates that the performance curve of these frames has increased compared to before and there has also been an increase in their ductility (Yang et al., 2009). Hedayat and Celikag assessed the stiffness and ductility of RBS connections. In their study, post-Northridge connections were modelled, and their behavior was evaluated. After the assessment, the location of plastic hinge formation was observed to move further from the column. Also, the plastic tension and strain concentration in the beam flanges decreased when using RBS connections (Hedayat and Celikag, 2009). Han et al. conducted studies resulting in methods for designing these connections which were more optimized compared to FEMA 350 (Han et al., 2009). Montuori

and Sagarese proposed an idea regarding the use of RBS in which a rigorous analysis is developed in order to assure the protection of the steel connections and all intermediate sections of the wooden beam (Montuori and Sagarese, 2018). A new scheme consisting of steel moment connections shared by flange cover-plate strengthening and web opening weakening was presented by Zhang et al. Some steel connections with different forms (standard connection, cover-plate reinforced connection, web-opening weakened connection, and equal strong (ES) connection) were tested under cyclic loading. The feasibility of the ES connection was verified to provide practical design applications (Zhang et al., 2019). In another study, a formulation was developed by Fanaie et.al. to evaluate the amount of stiffness variation or amplified elastic drift introduced by RBS connections in steel moment frames. Two simple, linear, and functional amplification factors of elastic story drift formulas for story beams with RBS connections are proposed for designers. The scope of these formulas will be expanded to plate girders as well (Fanaie et.al., 2019).

In this study, radiused cuts in the flange and slotted holes in the web of the connection beams were selected for retrofitting of the steel connections. These connections were designed and retrofitted based on recently optimized methods that were presented in the last decades. Cyclic behavior, energy dissipation levels, and connection ductility before and after retrofitting were evaluated and compared using nonlinear dynamic analysis.

## 2. DESIGNING THE MODELING

An 18-story steel building was designed with a special moment frame in one direction and high-ductility bracing in another direction. The plan of the building is shown in figure 1. Story height is 4 meters. The beams and columns were modeled based on W-sections. The steel type used is ST37. LRFD specification and AISC seismic provisions were used to design the building. The models were loaded according to ASCE 7-10.

After designing the beams and columns, the connections were modeled in the ANSYS platform. *Shell43* element was used, which takes up less calculation compared to solid elements, to carry out the nonlinear analysis of the connections. Stress distribution in the web and flanges of the beams was factored into the finite element model (FEM). Steel yielding and ultimate stress were considered to be  $2400 \frac{kgf}{cm^2}$  and  $3700 \frac{kgf}{cm^2}$ , respectively. To model the welding material, yielding tension of 3500 and ultimate tension 4200 were applied. The stress-strain curves of steel materials in the members and the weld are illustrated in figure 2.

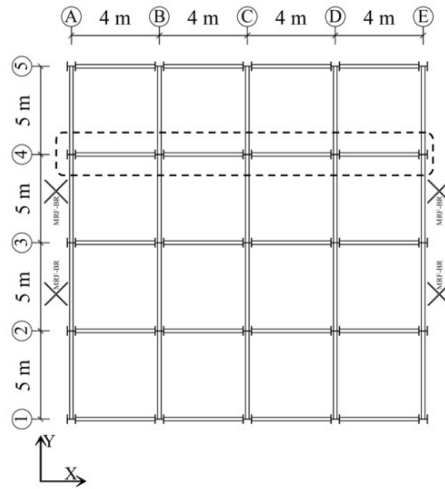


Fig. 1. Plan of the investigated building

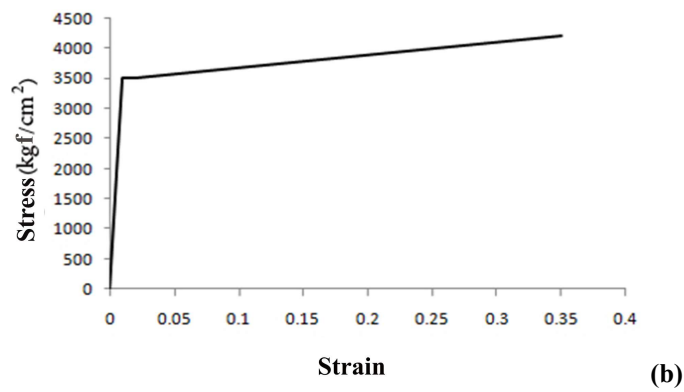
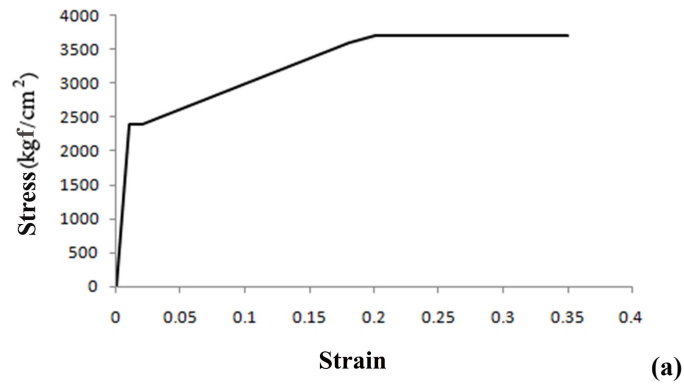


Fig. 2. The stress-strain curve of the steel materials in (a) members (b) weld

### 3. FINITE ELEMENT METHOD VERIFICATION

The experimental test done by Yang et. al (2009) was modeled in ANSYS to verify the FEM. Table 1 shows the characteristics of the properties of the W-section in connections in the experimental model.

Table 1. Beams and Columns Properties

Section	$b_f$ (mm)	$t_f$ (mm)	$h$ (mm)	$tw$ (mm)
Beam	200	12	400	8
Column	300	16	450	12

The test setup and dimensions of the beam and column are shown in figure 3. This experimental test included dynamic and static steps. The dynamic test was based on seismic response and the static test was based on failure mode in the frame. The N-S component of the El-Centro earthquake and the E-W components of the Northridge earthquake were selected for dynamic analysis. The loading displacement corresponding to the first mode was selected for static analysis.



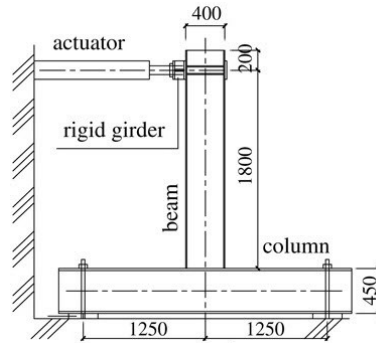


Fig. 3. Test Setup (Yang et. al., 2009)

In order to verify the finite element model for retrofitting, a 105mm wide hole where its closest edge was located 385 mm away from column side was applied. Figure 4 depicts the FE model of the specimen and meshed areas around the opening. FE model loading was a replicate of the loading in the experimental model.

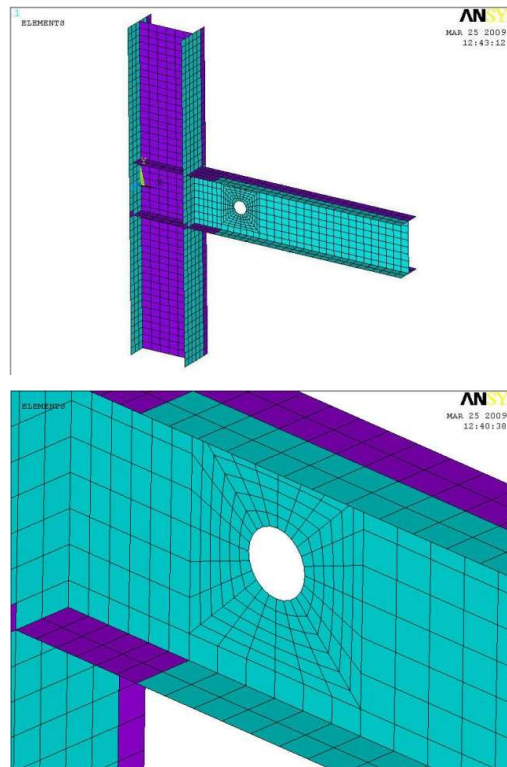


Fig. 4. FE model and meshing around the connection zone

The performance curves of the analyzed model were put together with those of the experimental specimen in Figure 5. According to figure 5, the FE model correlated well with the experimental specimen. The slight differences appearing in displacements larger than 20mm were mainly because the steel had reached yielding point at this stage.

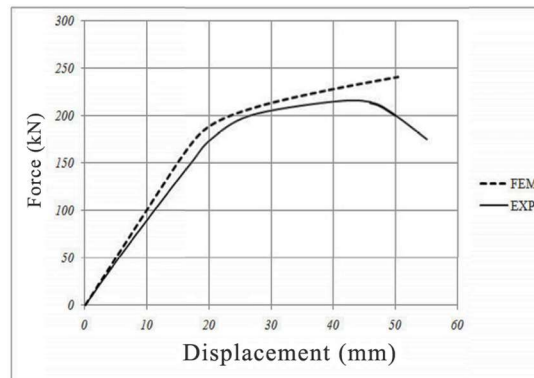


Fig. 5. comparison of the force-displacement curve of the experimental and analytical models

#### 4. RETROFITTING THE CONNECTIONS

In many cases, an opening in the beam web instead of the flange is used for reduced beam sections. These types of connections call for a rather large hole to reduce the tension in the weld connecting the web to the flanges. Due to the compound effect of shear and moment at the residual T-shape sections at the top and bottom of the hole, the failure occurs here first and before it happens in the beam flange. The retrofitted connections with a hole in the web were designed according to FEMA 350 and Yang et. al (2009). The retrofitted connections with radiused cuts in the flange were designed according to FEMA 350 and Han et.al (2009). The continuity plate used to model the panel zone had a thickness equal to the beam flange. Two extra plates were applied for better strength of the panel zone.

##### 4.1. Using long slotted hole in web

The first suggested section in this study for retrofitting is to use two long-slotted holes in the beams' web. Figure 6 shows the details of the retrofitted connection.

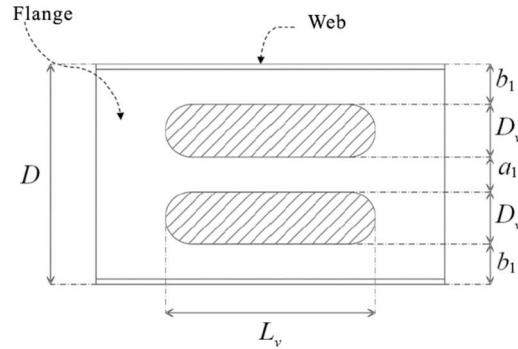


Fig. 6. RBS connection parameters with long-slotted holes

In which,  $L_v$  is the length of the slot along the beam's longitudinal direction which is equal to the space between the beginning and end of the slot,  $D_v$  is the depth of the slot,  $a_1$  is the net distance between two slots,  $D$  is the distance between slot center and column surface which is equal to beam height.  $a_1$  is obtained from equation 4.1.

$$a_1 = \frac{4.444 \times Z_b}{L \times b \times t_w} \quad (4.1)$$

$Z_b$  is the plastic module of the section and  $L$  is the length of the beam.  $t_w$  is the column web's thickness.  $L_v$  is determined from the following equation.

$$L_v = \alpha \times D \quad (4.2)$$

Parameter  $b_1$ , which is the distance between the beam flange and the top edge of the hole, can be calculated by equation 4.3:

$$b_1 = \beta \times c \quad (4.3)$$

In which  $c$  is the radius of the flange cut. Parameters  $\alpha$  and  $\beta$  are 0.75 and 2, respectively.  $r_v$  is the end radius of the slot which can be calculated using equation 4.4.

$$r_v(\text{mm}) = (D_v - 20\text{mm})/2 \quad (4.4)$$

Beam dimensions and the characteristics of the slot in the first retrofitted specimen are given in table 2. The loading applied to connections was according to FEMA 350 which are depicted in table 3.

Table 2. Properties of the RBS connection with long-slotted holes in the web

Beam	Column	$L_v(\text{mm})$	$c(\text{mm})$	$b_1(\text{mm})$	$D(\text{mm})$	$D_v(\text{mm})$
$W_{24 \times 68}$	$W_{14 \times 120}$	452	27	54	602	180

Table 3. Loading protocol

Stage	Maximum rotation (rad)	Maximum displacement (mm)	Loading cycle numbers
1	0.00375	7.5	6
2	0.005	10	6
3	0.0075	15	6
4	0.01	20	4
5	0.015	30	2
6	0.02	40	2
7	0.03	60	2

The strain distribution of the plastic hinge at maximum displacement is displayed in figure 7.

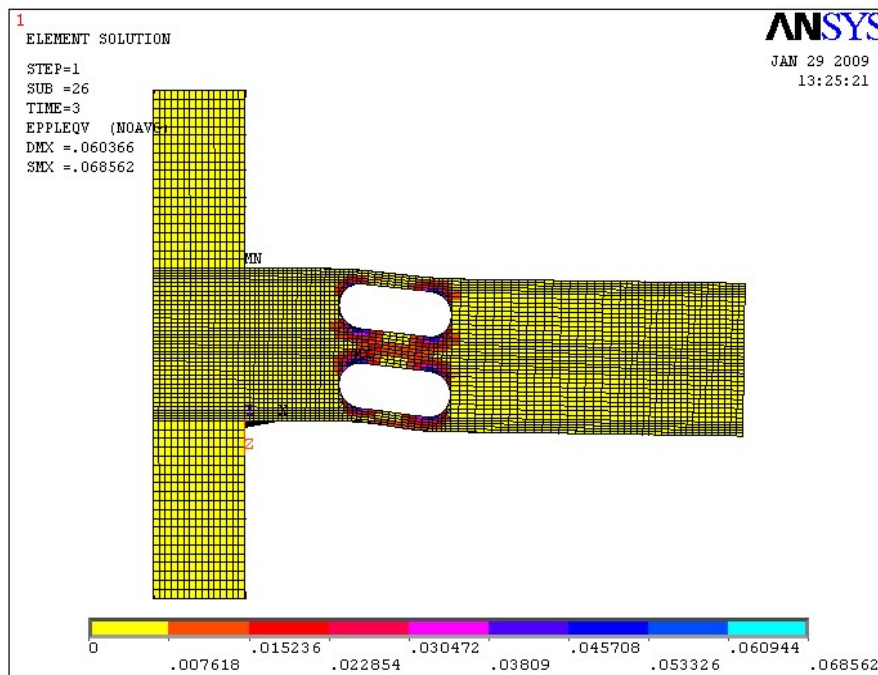


Fig. 7. Plastic strain distribution at 66mm displacement

According to the results, the first yielding point in this connection occurred in the slots area and at a displacement of 7.5 mm. The yielding zone was moved away from the columns side to zones near the long-slotted holes.

#### 4.2. Using radiused cut in the flange

The second suggested section for retrofitting the connections involved applying a radiused cut in the flange of the beam. The details of the suggested retrofitted connection are shown in figure 8. If the beam length is more than 10 times its height, this pattern is not recommended for retrofitting connections.

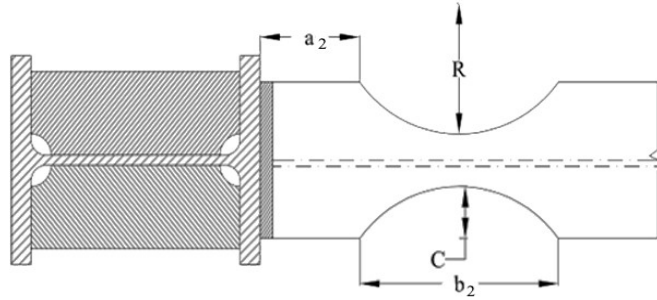


Fig. 8. RBS parameter with radiused cuts in the flange

Designing this type of connection consists of two steps. The first step is to determine the location of the reduced flange section according to equations 4.5 and 4.6.

$$a_2 \cong (0.5 \text{ to } 0.75)b_f \quad (4.5)$$

$$b_2 \cong (0.65 \text{ to } 0.85)d \quad (4.6)$$

In this equation,  $b_f$  is the beam flange thickness and  $d$  is the beam height. In the second step, the reduced cut depth ( $C$  parameter) is calculated using equation 4.7 and the radius of the cut in the section is calculated according to equation 4.8.

$$C \cong (0.2b_f \text{ to } 0.25b_f) \quad (4.7)$$

$$R = \frac{4C^2 + b^2}{8C} \quad (4.8)$$

These two shear amounts can be calculated using equations 4.9 and 4.10. In addition, the location of plastic hinge formation in RBS connections can be calculated using equation 4.11.

$$V_{pz} = \sum \left( \frac{M_{yb}}{d_b - t_{fb}} \right) \left( \frac{L}{L - d_c} \right) \left( \frac{h - d_b}{h} \right) \quad (4.9)$$

$$V_y = 0.55F_y d_c t_{cw} \left( 1 + 3 \frac{b_c t_f^2}{d_b d_c t_{cw}} \right) \quad (4.10)$$

$$S_h = \frac{d_c}{2} + \frac{b}{2} + a \quad (4.11)$$

In which  $F_y$  is the steel yielding stress at the panel zone,  $d_c$  is the column section height,  $t_{cw}$  is the panel zone thickness,  $t_f$  is the beam flange thickness, and  $d_h$  is the beam section height. Also,  $L$  is the beam span,  $h$  is the column height, and  $M_{yb}$  is the total moment applied to the column via the beam. Parameter  $S_h$  is the distance of the plastic hinge from the side of the column. The characteristics of the retrofitted connection with radiused cuts in the beam flange are summarized in table 4.

Table 4. Properties of the RBS connection with radiused cuts in the beam flange

Beam section	Column section	$a_2(mm)$	$b_2(mm)$	$c(mm)$	$R(mm)$
$W_{24 \times 68}$	$W_{14 \times 120}$	171	512	46	735

The applied load to this connection was also the same as the previous connection according to table 3. Figure 9 illustrates the maximum plastic strain distribution in the connection at maximum displacement.

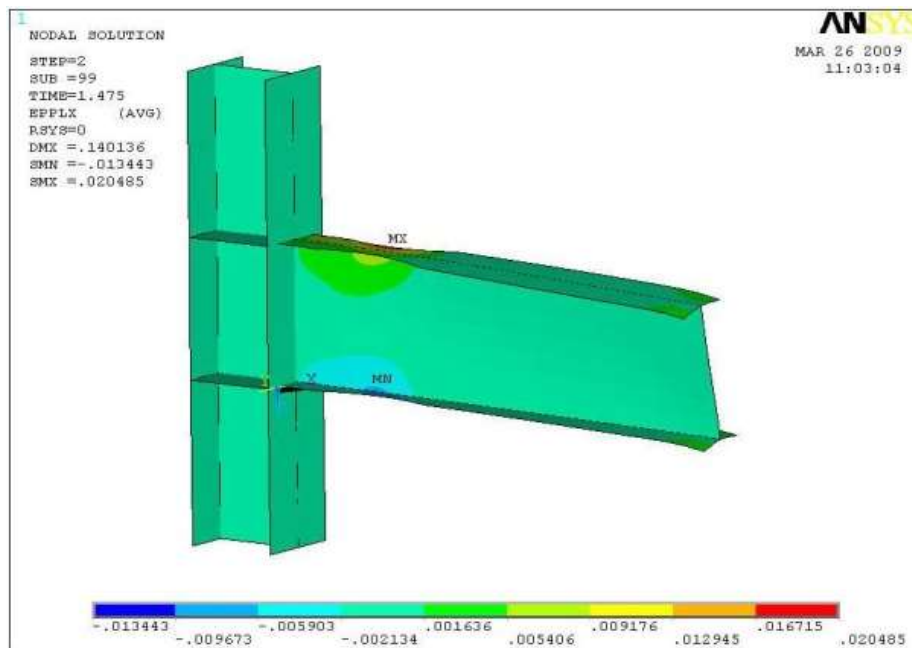


Fig. 9. Plastic strain distribution at maximum displacement

## 5. INVESTIGATING THE BEHAVIOR OF RETROFITTED CONNECTIONS

To compare the retrofitted connections, their behavior before and after the retrofitting was evaluated. The retrofitted connection with long-slotted holes in the web was indicated by A-Web. The retrofit connection with radiused cuts at the flange was indicated by A-Flange. The pre-retrofit connection was indicated by B-Non. The hysteresis behavior of the connections is shown before and after retrofit in figure 10 and table 5.

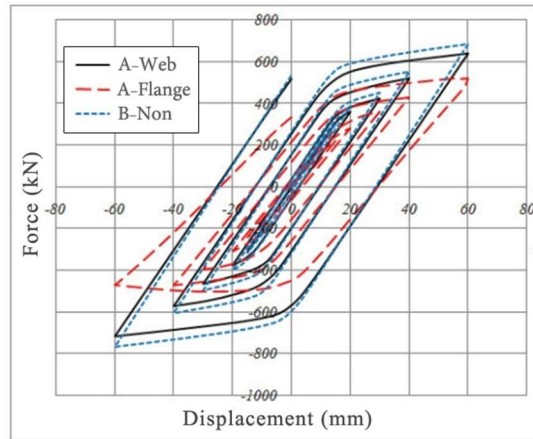


Fig. 10. connections' hysteresis curves

Table 5. Ductility and the area under the curves of specimens

Specimen	Yielding displacement $\Delta_y$ (mm)	Ultimate displacement $\Delta_u$ (mm)	Ductility $\mu = \Delta_u / \Delta_y$	The area under the hysteresis curve compared to B-Non	The area under the force-displacement curve compared to B-Non
A-Web	19	61	3.21	0.98	0.95
A-Flange	14	52.5	3.75	0.67	0.74
B-Non	21	66.5	3.17	1	1

The pre-retrofit specimen had a larger area under the curve compared to the other two specimens. According to the specification of ATC-24, the ductility index is defined as the ratio of ultimate displacement to required displacement to have the first yielding. The A-flange specimen had the highest ductility index compared to the other two specimens. The ductility index of the A-flange specimen was 16 and 17% more than the A-Flange and B-non specimens, respectively. The first yielding point of the A-Flange specimen happened at 14 mm displacement, which was lower by 26 and 33 % compared to the

A-Web and B-Non specimens, respectively. The earlier yielding point of the A-Flange compared to the other two specimens was due to the stress concentration around the circular parts of the long-slotted holes. The same phenomena occurring around the radiused cuts of the A-Web specimen also caused earlier yielding of this specimen compared to B-Non.

The performance curves of connections are compared in figure 11, before and after retrofitting.

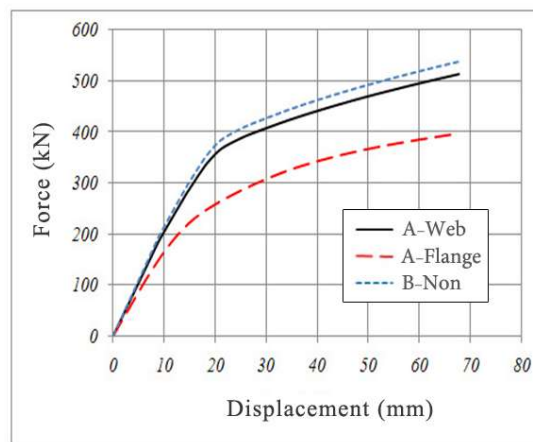


Fig. 11. Force-displacement curve of the connections

Diagrams of A-WEB and B-NON connections had a greater correlation because of similar behavior in the linear zone. The maximum plastic strain distribution based on displacement in the connections is illustrated in figure 12.

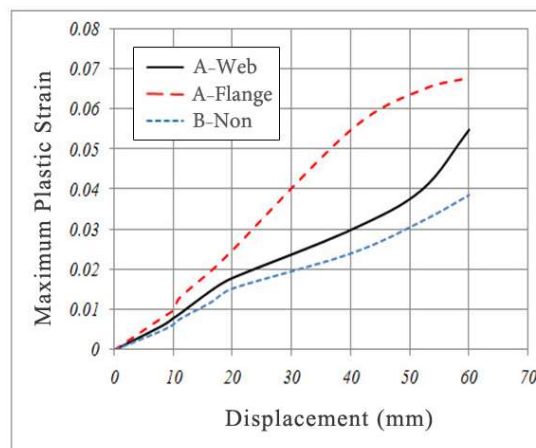


Fig. 12. The maximum plastic strain of specimens

The diagrams shown in figure 13 are a good index for comparison of plastic strain occurring in the sections. The difference between maximum plastic strain in the A-Flange connection at 60mm displacement was 24 and 79% more than the A-WEB and B-NON, respectively. The large difference in maximum plastic strain in the A-Flange specimen compared to A-WEB and B-NON occurred in the weakened section. An explanation for this could be the stress concentration at the radiused corners of the A-Web and A-Flange specimen, which resulted in higher strain.

The extent of energy dissipation in the web and flange of retrofitted beams are measured at different distances from the panel zone and displayed in figures 13 and 14.

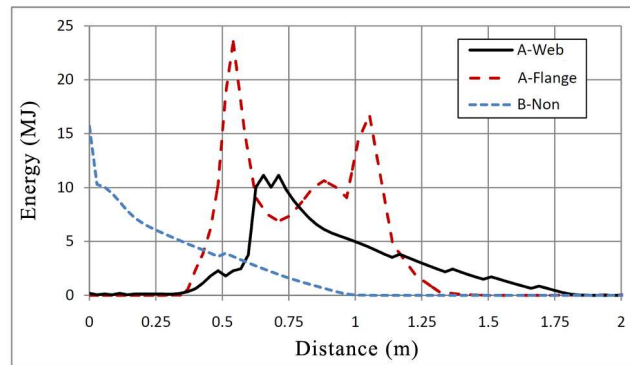


Fig. 13. Dissipated energy in beam flanges at different distances from the panel zone

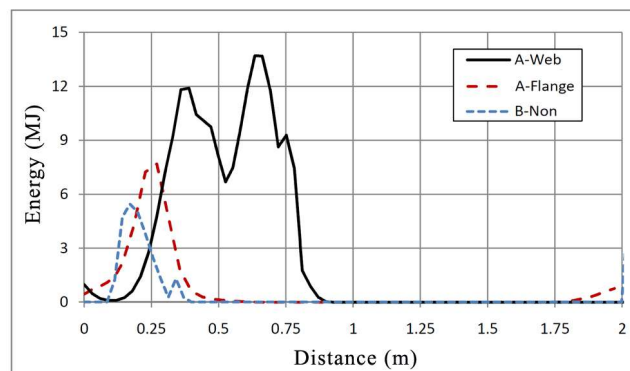


Fig. 14. Dissipated energy in beam web at different distances from the panel zone

The dissipated energy in the beam flanges was increased 31% for the A-Flange specimen and 34% for the A-Web specimen, after retrofitting. The dissipated energy in the beam web was increased 28% for the A-Flange specimen and 58% for the A-Web specimen, after retrofitting.

## 6. CONCLUSION

In this study, two models of retrofitted connections were compared. Their behavior before and after the retrofitting was evaluated. The first connection was retrofitted with a long-slotted hole in the web of the beam. The second connection was retrofitted with radiused cuts at the flange of the beam. Results showed that retrofitted connections with radiused cuts in the flange have better behavior by far in dissipating seismic energy compared to connections retrofitted with long-slotted holes in the web. The area under the hysteresis curves of the pre-retrofit specimen is 67 and 98% larger than the retrofitted specimen with long-slotted holes and with radiused cuts in the flange, respectively. The ductility index in the specimen with radiused cuts in the flange is greater than in the specimen with long-slotted holes in the web. Connections retrofitted with radiused cuts in the flange, when compared to long-slotted holes in the web, have much higher energy absorption although lower plastic strain levels. The maximum plastic strain at 60mm displacement for the retrofitted connection with long-slotted holes in the web, when compared to the radiused cut specimen, shows 80% reduction which indicates less plastic displacement in the radiused cut retrofitted connection. After retrofitting the connection, the dissipated energy in the beam flanges of the radiused cut specimen had a lower increment compared to the retrofitted connection with the long-slotted hole. The energy dissipation in the retrofitted beam web in the specimen with radiused cuts at the flange had a higher increment compared to the specimen with the long-slotted hole in the web.

## REFERENCES

1. AISC, Prequalified Connections for Special and Intermediate Steel Moment Frames for Seismic Applications. Chicago, Illinois, ANSI/AISC 358, 2016.
2. AISC, Specification for Structural Steel Buildings, Chicago, Illinois: ANSI/AISC 360, 2016.
3. ANSYS. Multiphysics 12.1. Canonsber: Ansys Inc, 2010.
4. ASCE 7-10, Minimum Design Loads for Buildings and Other Structures. American Society of Civil Engineers, Reston, Virginia, 2010.
5. ATC 24, Guidelines for Cyclic Seismic Testing of Components of Steel Structures, Applied Technology Council, 1992.
6. Bogdanovic, A, Rakicevic, Z, and Noroozinejad Farsangi, E 2019. Shake table tests and numerical investigation of a resilient damping device for seismic response control of building structures. *Structural Control and Health Monitoring*, 26(11), e2443.

7. Chi, B, Uang, CM and Chen, A 2006. Seismic rehabilitation of pre-Northridge steel moment connections: A case study. *Journal of Constructional Steel Research*, 62,783-792.
8. Fanaie, N, Faegh, SS and Partovi, F 2019. An improved and innovative formulation for calculating amplified elastic story drift induced by RBS connections in steel moment frames. *Journal of Constructional Steel Research*, 160, 510-527.
9. Farsangi, EN, Yang, TY and Tasnimi, AA 2016. Influence of concurrent horizontal and vertical ground excitations on the collapse margins of non-ductile RC frame buildings. *Structural Engineering and Mechanics*, 59(4), pp.653-669.
10. Farsangi, EN, Tasnimi, AA, Yang, TY, Takewaki, I and Mohammadhasani, M 2018. Seismic performance of a resilient low-damage base isolation system under combined vertical and horizontal excitations. *Smart Structures and Systems*, 22(4), pp.383-397.
11. FEMA-350, Recommended Seismic Design Criteria for New Steel Moment Frame Buildings, FEMA 350. Washington, DC: Federal Emergency Management Agency, 2000.
12. Gerami, M, Sharbati, Y and Sivandi-Pour, A 2013. Nonlinear seismic vulnerability evaluation of irregular steel buildings with cumulative damage indices. *International Journal of Advanced Structural Engineering*, 5, p.9.
13. Han, SW, Moon, KH and Stojadinovic, B 2009. Design equations for moment strength of RBS-B connections. *Journal of Constructional Steel Research*, 65, 1087-1095.
14. Hedayat, AA and Celikag, M 2009. Post-Northridge connection with modified beam end configuration to enhance strength and ductility. *Journal of Constructional Steel Research*, 65, 1413-1430.
15. Jones, SL, Fry, GT and Engelhardt, MD 2002. Experimental evaluation of cyclically loaded reduced beam section moment connections. *Journal of Structural Engineering*, 128(4), pp.441-451.
16. Lee, CH, Jeon, SW, Kim, JH and Uang, CM 2005. Effects of panel zone strength and beam web connection method on seismic performance of reduced beam section steel moment connections. *Journal of Structural Engineering*, 131(12), pp.1854-1865.
17. Montuori, R and Sagarese, V 2018. The use of steel rbs to increase ductility of wooden beams. *Engineering Structures*, 169, pp.154-161.
18. Rong, B, Liu, S, Yan, JB and Zhang, R 2018. Shear behaviour of panel zone in through-diaphragm connections to steel tubular columns. *Thin-Walled Structures*, 122, 286-299.
19. SAC joint venture. Recommended seismic design criteria for new steel moment-frame buildings; FEMA-350. Richmond, Calif, 2000.

20. Sivandi-Pour, A, Gerami, M and Kheyroddin, A 2015. Determination of modal damping ratios for non-classically damped rehabilitated steel structures. *Iranian Journal of Science and Technology. Transactions of Civil Engineering*, 39, p.81.
21. Sivandi-Pour, A, Gerami, M and Khodayarnezhad, D 2014. Equivalent modal damping ratios for non-classically damped hybrid steel concrete buildings with transitional storey. *Structural Engineering and Mechanics*, 50, pp.383-401.
22. Tuna, M and Topkaya, C 2015. Panel zone deformation demands in steel moment resisting frames. *Journal of Constructional Steel Research*, 110, 65-75.
23. Yang, Q, Li, B and Yang, N 2009. Aseismic behaviors of steel moment resisting frames with opening in beam web. *Journal of Constructional Steel Research*, 65, 1323-1336.
24. Zhang, X, Zheng, S and Zhao, X 2019. Seismic performance of steel beam-to-column moment connections with different structural forms. *Journal of Constructional Steel Research*, 158, 130-142.

*Editor received the manuscript: 11.11.2019*